

RSC Advances



This is an *Accepted Manuscript*, which has been through the Royal Society of Chemistry peer review process and has been accepted for publication.

Accepted Manuscripts are published online shortly after acceptance, before technical editing, formatting and proof reading. Using this free service, authors can make their results available to the community, in citable form, before we publish the edited article. This *Accepted Manuscript* will be replaced by the edited, formatted and paginated article as soon as this is available.

You can find more information about *Accepted Manuscripts* in the [Information for Authors](#).

Please note that technical editing may introduce minor changes to the text and/or graphics, which may alter content. The journal's standard [Terms & Conditions](#) and the [Ethical guidelines](#) still apply. In no event shall the Royal Society of Chemistry be held responsible for any errors or omissions in this *Accepted Manuscript* or any consequences arising from the use of any information it contains.

A new fluorescence and colorimetric sensor for highly selective and sensitive detection of glucose in 100% water

Yuming Shen,^{ab} Xiangyang Zhang,^{*a} Xi Huang,^b Youyu Zhang,^{*b} Chunxiang Zhang,^a Junling Jin,^a Xuewen Liu,^a Haitao Li,^b and Shouzhuo Yao^b

^a College of Chemistry and Chemical Engineering, Hunan University of Arts and Science, ChangDe, 415000, PR China E-mail: zhangxiangy06@163.com

^b Key Laboratory of Chemical Biology and Traditional Chinese Medicine Research (Ministry of Education), College of Chemistry and Chemical Engineering, Hunan Normal University, Changsha 410081, PR China E-mail: zhangyy@hunnu.edu.cn

Abstract

A new naphthalimide derivative containing hexanoic acid and boronate groups was designed and synthesized. The compound displays off / on ratio signals, highly selective and sensitive towards glucose based on naphthalimide derivative reacting with enzyme generated H_2O_2 in 100% water. The fluorescence intensity is proportional to the concentration of glucose over a range of 0-120 μM ($R^2 = 0.9912$), with a limit of detection of 0.3 μM ($S / N = 3$). Moreover, the fluorescent sensor has been used for determination of glucose in serum with satisfactory results, which further demonstrates its value of practical applications.

Keywords: Glucose; Fluorescent probe; Naphthalimide derivative; Glucose oxidase

1. Introduction

Glucose plays important roles in a diverse range of biological processes and is a basic necessity of living organisms [1]. An irregular concentration of glucose in human blood can cause biological dysfunctions, such as dry skin, blurred vision, extreme thirst, slow wound healing and drowsiness [2]. Furthermore, high levels of blood glucose are warning signals of type-2 diabetes, hypertension, and cardiovascular disease [3-4]. Therefore, many research interests have been directed to developing reliable techniques for determination of glucose in order to understand its chemical and biological function in certain physiological and pathological events [5].

Owing to the advantages of high sensitivity, inherent simplicity, rapid detection, inexpensive instrumentation and suitable for biological systems, fluorimetric glucose sensors have received considerable attention [6-7]. Fluorimetric sensors for directly detection of glucose are mainly based on boronic acid due to the covalent binding properties of boronic acid with the diol group of sugars [8-9]. However, many reported fluorimetric glucose sensors based on boronic acid derivatives faced many problems such as the interference of other saccharides especially fructose, working at high pH aqueous solution and poor selectivity [10-11]. It was shown that aryl phenylboronic ester or phenylboronic acid can selectively react with H_2O_2 to produce a phenolic group [12]. Taking advantage of the highly specificity and efficiency of glucose oxidase (GOx) enzyme, a few fluorogenic glucose sensing based on glucose oxidase (GOx) enzyme and boronic ester derivatives have been developed [13].

This method overcomes the disadvantage of using a boronic-based fluorescence sensor for detection of glucose. However, most of probes for detecting H_2O_2 have poor water-solubility, and they are only operable in water-organic solvent mixtures [14-15]. These drawbacks have limited their combination with glucose oxidase (GOx) enzyme because of most of enzymes can only work well in 100% water solution and water-organic solvent mixtures sometimes even make them inactivate [16]. Furthermore, they could not be applied in real biological systems. Significantly, the fluorescent probe for H_2O_2 is privileged with good water-solubility. In general, water-soluble fluorescent probes can be obtained *via* introduction of quaternary ammonium salt fragments or sulfonic acid groups. In this way, a few water-soluble fluorescent glucose probes have been developed. For example, Zhang and coworkers reported a highly selective fluorescence turn-on detection of hydrogen peroxide and D-glucose based on the aggregation/deaggregation of a modified tetraphenylethylene bearing boronic ester and pyridinium fragments [17]. Feng et al. reported a water-soluble sulfonated porphyrin fluorescence sensor for turn-off detection of H_2O_2 and glucose [18]. Although those sensors based on GOx can selectively detect glucose in 100% water, there are still encounter some problems, such as complicated synthetic procedures and low sensitivity. These limitations retarded the application of the probe in real biological. On the other hand, fluorescence approaches for detection of glucose based on nanoparticles have been developed, such as Si-dots [19], gold nanoclusters [20] and CdTe quantum dots [21]. These methods are highly sensitive and selective. However,

they always suffer from potential chemical instability and toxicity. Therefore, it is eagerly to design and develop a highly sensitive and selective, simple and water-solubility fluorescent probes for detection glucose.

1, 8-naphthalimide fluorophores, large conjugated and coplanar, have the advantage of moderate fluorescence emission wavelength and large stokes shift and high fluorescence quantum yield [22-23]. Moreover, hexanoic acid as a hydrophilic group can make naphthalimide derivatives at imide moieties operate in aqueous solution [24]. However, to the best of our knowledge, fluorimetric glucose sensors bearing 1, 8-naphthalimide fragment, boronate and carboxylic acid groups have rarely been reported. It is still a challenge to synthesis those sensors.

Based on the advantages of 1, 8-naphthalimide fluorophores, we designed a sensitive 1, 8-naphthalimide fluorophore containing hexanoic acid group and boronate with a significant spectral shift (from 445 nm to 557 nm) for H_2O_2 . The probe selected 1, 8-naphthalimide as the fluorophore and the boronic ester as a recognition unit. The boronate moiety is attached to the fluorophore of 1, 8-naphthalimide, upon reaction with H_2O_2 , hydrolytic deprotection of the boronates would subsequently generate fluorescent fluorescein product. Hexanoic acid group can make naphthalimide derivatives operate in 100% water solution. It results in an increase in fluorescence and a “turn-on” signal in 100% water solution. The novel 1, 8-naphthalimide fluorophore sensor is highly sensitive and selective toward GOx enzyme-generated H_2O_2 in aqueous solution. Moreover, it's worth noting that our designed sensor can colorimetric and fluorescence detect glucose in 100% water solution and it is

very suitable for real application. Moreover, it's worth noting that our designed sensor can colorimetric and fluorescence detect glucose in 100% water solution. A dual-signaling chemodosimeter can combine the sensitivity of fluorescence with the convenience and esthetic appeal of a colorimetric assay [25-26], and it is very suitable for real application.

2 Experimental

2.1 Reagents and chemicals

4-Bromo-1, 8-naphthalic anhydride, 6-aminohexanoic acid, bis(pinacolato)diboron, [1,1'-Bis(diphenylphosphino)ferrocene] palladium(II) dichloride dichloromethane were purchased from Sigma-Aldrich company. Sucrose, fructose, lactose, mannose, arabinose, citric acid, ascorbic acid, aspartate, arginine, proline, histidine were purchased from Aladin Ltd. (Shanghai, China). All other chemicals used in this work were of analytical grade, purchased from Sinopharm chemical reagent company and used without further purification. The synthesis of compound **2** was similar to the procedures reported by Minyong Li et al [27]. The thin-layer chromatography (TLC) was carried out on silica gel plates (60F-254) using UV-light to monitor the reaction, and silica gel (200-300 mesh) was used for column chromatography. Milli-Q ultrapure water (Millipore, ≥ 18 M cm) was used throughout.

2.2 Instrumentation

UV-Vis absorption spectra were recorded with a UV2450 (Shimadzu Co., Japan). Fluorescence measurements were carried out on an F-4500 FL spectrophotometer (Hitachi Ltd, Japan) with excitation slit set at 10 nm and emission at 10 nm. All pH

measurements were made with a Sartorius basic pH-meter PB-10. ^1H NMR measurements were performed on a Bruker AVB-500 MHz NMR spectrometer (Bruker biospin, Switzerland). MS analysis was performed on an Agilent 1100 series mass spectrometer and electrospray ionization high-resolution mass spectra (Bruker P-SIMS-GlyFT-ICR).

2.3 The synthesis of compound 1

Under the protection of argon, a mixture of **2** (0.32g, 1 mmol), 6-aminohexanoic acid (0.26 g, 2 mmol) and anhydrous ethanol (5 mL) was stirred at 90°C for 12 h. Then, the solvent was removed by rotary evaporation and the residue was purified by silica gel column chromatography (CH_2Cl_2 / CH_3OH , 20:1, V/V) to afford a white solid in 93% yield (0.41 g). ^1H NMR (500 MHz, CDCl_3) δ (ppm): 9.10 (d, J = 8.5 Hz, 1H), 8.59 (d, J = 7.0 Hz, 1H), 8.55 (d, J = 7.0 Hz, 1H), 8.28 (d, J = 7.0 Hz, 1H), 7.76 (d, J = 8.5 Hz, 1H), 4.18 (t, J = 7.5 Hz, 2H), 2.38 (t, J = 7.5 Hz, 2H), 1.71 - 1.78 (m, 4H), 1.47 - 1.52 (m, 2H), 1.45 (s, 12H); ^{13}C NMR (125 MHz, CDCl_3) δ (ppm): 178.3, 164.3, 164.3, 135.8, 135.3, 135.0, 131.3, 131.0, 129.9, 127.9, 127.1, 127.0, 124.7, 84.6, 40.2, 33.7, 27.7, 26.6, 25.0, 24.4; ESI-MS calcd for $\text{C}_{24}\text{H}_{28}\text{BNO}_6$ $[\text{M}+1]^+$ 438.2932, found 438.2082.

2.4 Measurement procedure

PBS buffer solutions (50 mM, pH = 7.0) were prepared in deionized water. Compound **1** was dissolved in the requisite amount of PBS buffer solutions (50 mM, pH = 7.0) as a stock solution (200 μM). The solutions of various biologically species were diluted with PBS buffer solution (50 mM, pH = 7.0). The pH solutions were

obtained by adjustment of PBS buffer solution (50 mM, pH = 7.0) with 1 mM HCl or 1 mM NaOH. The glucose were carried out as follows: the ensemble PBS buffer (50 mM, pH = 7.0) containing 5 μ M compound **1**, 10 μ g / mL GOx, and different amounts of glucose (0-500 μ M) were equilibrated under gentle shaking at 37 $^{\circ}$ C for 20 min. The fluorescence intensity was recorded with the emission from 490 to 660 nm at excitation of 445 nm.

2.5 Determination of glucose from serum samples

Serum samples were diluted 100-folds with PBS buffer solution (50 mM, pH = 7.0). Before analysis, aliquots of PBS buffer containing 10 μ g/mL GOx and 5 μ M compound **1** were equilibrated under gentle shaking at 37 $^{\circ}$ C for 1 h.

3 Results and discussion

3.1 Synthesis of compound **1**

(Preferred position for scheme 1)

Compound **1** was synthesized according to the synthetic route outlined in Scheme 1. Palladium-catalyzed Suzuki coupling reactions between 4-bromo-1, 8-naphthalic anhydride and bis(pinacolato)diboron yielded compound **2**, which was allowed to react with 6-aminohexanoic acid to afford compound **1**. The chemical structure of compound **1** was characterized with 1 H NMR, 13 C NMR and mass spectra and presented in the supplementary materials (Figs.S5-S7). In addition, during the course of the experiment, we found that first introduce carboxylic acid group to naphthalimide derivatives can not obtain compound **1**.

3.2 Spectra properties of compound **1**

As expected, compound **1** is soluble in water, and the PBS buffer solution (50 mM, pH = 7.0) of compound **1** (5 μ M) can be easily prepared. Moreover, the H_2O_2 would convert boronic ester of the fluorescence sensor to the phenol in water solution. Thus, we first examined the reaction of the probe with H_2O_2 (Fig. 1). As is seen, compound **1** itself has a strong absorption band at 350 nm. However, in the presence of H_2O_2 , the absorption peak at 350 nm decreased and a new absorption peak at 445 nm occurred. The bathochromic-shift of the absorption wavelength is reflected in a change in the color of the solution (from colorless to yellow), which is easily detectable by naked eye under visible light. As shown in Fig. 1B, on excitation at 445 nm, compound **1** has weak fluorescence in the presence of H_2O_2 . However, compound **1** has strong emission at 557 nm, and the normalized fluorescence intensity is increased with the increase of H_2O_2 concentrations. Those suggested that the optical of compound **1** can change upon direct addition of H_2O_2 .

(Preferred position for Fig. 1)

3.3 Mechanism of the detection of glucose

H_2O_2 is generated using glucose and glucose oxidase. H_2O_2 reacts with compound **1** to produce the fluorescent sensor. By recording the change fluorescence intensity of the system, the concentration of glucose can be measured. The general process for detection of glucose based on compound **1** is shown in Scheme 2. To test this, normalized fluorescence of compound **1** containing glucose in the absence and in the presence of GOx were investigated in Fig. 2. As depicted in Fig. 2, compound **1**

displayed no change of the normalized fluorescence intensity at 557 nm in the absence of GOx. When GOx was added, the fluorescence intensity of compound **1** was obviously increased. These results indicated that glucose is oxidized by GOx to produce H₂O₂, and H₂O₂ causes the change of fluorescence intensity. To further clarify the sensing mechanism of compound **1**, the purified product of the reaction of compound **1** with H₂O₂ was then characterized by ¹H NMR and mass spectra (Figs. S8–S9). From ¹H NMR, the peak of boronic ester group (δ = 1.45 ppm, 12H) completely disappeared and from MS, a new mass-to-charge ratio ($m/z = 326.17$, [M-H]⁻, negative ion mode) appeared. The results indicated the boronic ester group has been converted to the phenol group by the H₂O₂.

(Preferred position for Fig. 2)

(Preferred position for scheme 2)

3.4 Optimization of detection conditions

(Preferred position for Fig.3)

(Preferred position for Fig. 4)

The amount of the H₂O₂ production is controlled by GOx. Thus, we firstly investigated the effect of concentrations of GOx. Fig. 3 shows the relative fluorescence intensity of compound **1** on interaction with 120 μ M glucose and different ratios of GOx. It can be seen that a gradual increase of the fluorescence was observed with increasing concentrations of GOx at 557 nm. Meanwhile, the

emission intensity reached plateau when 10 $\mu\text{g/mL}$ GOx was added. Therefore, 10 $\mu\text{g/mL}$ GOx was selected as the following experiments.

To study the practical applicability, the effects of pH on the fluorescence response of compound **1** including GOx in the presence of glucose were investigated (Fig. 4). Fig. 4 displayed the relative fluorescence intensity of the compound **1** distinct fluorescence changes under different pH conditions. The fluorescence intensity of probe is very feeble in at pH 1.0-3.0. However, when the solution pH is between 4.0 and 7.0 or in the range of 7.0-11.0, a small fluorescence increase was induced in the presence of glucose including GOx. At pH 7.0, the optimal fluorescence signal response was detectable. This indicated that compound **1** could be used to detect g around biological pH condition.

Reaction time is also an important factor for reaction-based probes, and the time-dependent fluorescence spectra of compound **1** including GOx in the presence of glucose investigated (Fig. 5). Fig. 5 showed that the relative fluorescence intensity enhanced with the increasing reaction time at 557 nm and the fluorescence intensity reached the equilibrium within 20 min. Therefore, 20 min was chosen as the optimal reaction time in this work.

To effectively detect glucose by enzymatic mechanism of GOx and glucose, the effects of temperature was also investigated (Fig. 6). As shown in Fig. 6, the relative fluorescence intensity of compound **1** changes with temperature. At 37°C the relative fluorescence intensity of compound **1** was the highest. The results could be correlated decomposition rate of H_2O_2 and with the enzyme kinetics. Thus, 37°C was selected as

reaction temperature in the further experiments.

(Preferred position for Fig. 5)

(Preferred position for Fig. 6)

3.5 Selective response of compound **1** to glucose

To study the compound **1** as a highly selective chemosensor for glucose, various sugar and biologically relevant species were examined. As shown in Fig. 7, the addition of 120 μM sugar (sucrose, fructose, lactose, mannose, arabinose), amino acids (citric acid, ascorbic acid, aspartate, arginine, proline, histidine), metal ions (Na^+ , Mg^{2+} , Ca^{2+}) to the solution of compound **1** (5 μM) caused nearly no changes in the relative fluorescence intensity at 557 nm. However, the fluorescence of compound **1** response appeared when the glucose was introduced. Moreover, other sugar did not affect the glucose detection under the enzymatic GOx mechanism. The results indicate that compound **1** can only react with glucose including GOx and it is a reliable highly selective sensor for glucose.

(Preferred position for Fig.7)

3.6 Detection of glucose

Under the optimal conditions, detection of glucose was investigated. In Fig. 8, the relative fluorescence intensity titration of compound **1** including glucose oxidase by different amounts of glucose was described. With increasing the glucose concentration, the relative fluorescence intensity at 557 nm is gradually increased. A visual fluorescence change (from colorless to green) of compound **1** demonstrates that

compound **1** can be used conveniently as a “naked-eye” fluorescence indicator for glucose. The relative fluorescence intensity of compound **1** also showed a good linear response ($R^2 = 0.9912$) in the range of 0 to 120 μM . The detection limit for glucose was estimated to 0.3 μM ($S / N = 3$). Furthermore, the UV spectrum of compound **1** containing glucose in the absence and in the presence of GOx were investigated (see ESI†, Fig. S1). As depicted in Fig. S1, similar absorption spectra change was displayed to that with H_2O_2 . Therefore, compound **1** can serve as a “naked-eye” indicator for glucose under visible light. In comparison with other methods (Table 1), compound **1** has its advantage over other reported glucose determination methods. Therefore, the fluorescent probe has great potential for practical applications.

(Preferred position for Fig. 8)

(Preferred position for Table 1)

3.7 Detection of glucose in real samples

The high selectivity and sensitivity sensor for glucose indicated that it could be applied to detect glucose in real samples. In order to investigate the analytical application of this spectrofluorometric method, the probe was applied to detect glucose in serum (Table 2). Table 2 shows the recoveries of the samples were in the range of 93.7% to 104.3% with the RSD in 5.0%. Moreover, the probe was employed to detect glucose levels in urine samples spiked with glucose (see ESI†, Table S1). Table S1 displays the recoveries

were acceptable. These results suggested that the compound **1** was capable of fluorescence sensing of glucose in real samples.

(Preferred position for Table 2)

3.9 Theoretical calculation

To better understand the optical responses of compound **1** to H₂O₂, we carried out density functional theory (DFT) calculations at the B3LYP/6-31G (d, p) level of the Gaussian 09 program. As displayed in Table S2 (see ESI[†]), the calculated main absorption peaks of compound **1** and **1**-H₂O₂ reaction product in water is 359 nm and 445 nm, respectively. The results are well agreement with the experimentally observed adsorption spectra. As shown in Table S3 (see ESI[†]), the TD-DFT calculations confirmed that the S₁→S₀ (HOMO→LUMO, oscillator strength $f = 0.346$) and S₁→S₀ (HOMO→LUMO, oscillator strength $f = 0.126$) electronic transitions are considered to be the allowable transitions for compound **1** and **1**-H₂O₂ reaction product, respectively. Thus, the electron distributions in HOMO and LUMO for compound **1** and **1**-H₂O₂ reaction product are displayed in Fig. 9. For compound **1**, both the HOMO and LUMO are localized on the entire molecule. Upon excitation, almost no electron transfer process will take place on compound **1**. Accordingly, compound **1** exhibited dark fluorescence. However, in the **1**-H₂O₂ reaction product, the HOMO→LUMO transition was the electron redistributions from oxygen anion to naphthalimide group. Upon excitation, some degree of ICT process will occur from the oxygen anion to naphthalimide group. Therefore, the **1**-H₂O₂ reaction product will be highly fluorescent.

(Preferred position for Fig. 9)

4. Conclusion

In summary, a novel colorimetric/fluorescence dual-channel sensor was designed and synthesized based on naphthalimide derivative. The probe can highly selectivity and sensitivity detect glucose in 100% water, which is attributed to the reaction between compound **1** and enzyme-generated H₂O₂. In addition, compared with probe previously reported for detection of glucose, the probe has the advantages of good selectivity, low detection limit and water-solubility. Furthermore, this strategy may become a promising way for glucose detection in biological samples.

Acknowledgments

This work was supported by the National Natural Science Foundation of China (21342012, 21375037), Hunan Provincial Natural Science Foundation of China (11JJ3023, 15JJ3094), Science and Technology Department (13JJ2020), State Key Laboratory of Chemo/Biosensing and Chemometrics Foundation (KLCBTC MR 2011-05), and Scientific Research Fund of Hunan Provincial Education Department (13C635).

References

- 1 Y. Minokoshi, C. R. Kahn and B. B. Kahn, *J. Biol. Chem.*, 2003, **278**, 33609-33612.
- 2 D. Giugliano, R. Marfella, L. Coppola, G. Verrazzo, R. Acampora, R. Giunta, F. Nappo, C. Lucarelli and F. D'Onofrio, *Circulation*, 1997, **95**, 1783-1790.
- 3 (a) J. Lawton, D. Rankin, D. D. Cooke, M. Clark, J. Elliot and S. Heller, *Diabetes Res. Clin. Pract.* 2011, **91**, 87-93; (b) Y. Teramura, L. N. Minh, T. Kawamoto and

- H. Iwata, *Bioconjugate Chem.* 2010, **21**, 792-796.
- 4 J. S. Wu, Y. H. Peng, J. M. Wu, C. J. Hsieh, S. H. Wu, M. S. Coumar, J. S. Song, J. C. Lee, C. H. Tsai, C. T. Chen, Y. W. Liu, Y. S. Chao and S. Y. Wu, *J. Med. Chem.* 2010, **53**, 8770-8774.
- 5 (a) E. Vezouvioun and C. R. Lowe, *Biosensors and Bioelectronics*, 2015, **68**, 371-381; (b) L. Li, F. F. Gao, J. Ye, Z. Z. Chen, Q. L. Li, W. Gao, L. F. Ji, R. R. Zhang and B. Tang, *Anal. Chem.* 2013, **85**, 9721-9727.
- 6 D. Odaci, B. N. Gacal, B. Gacal, S. Timur and Y. Yagci, *Biomacromolecules*, **2009**, **10**, 2928-2934.
- 7 K.-B. Oha and H. Matsuoka, *International Journal of Food Microbiology*, 2002, **76**, 47-53.
- 8 C. S. Lim, C. Chung, H. M. Kim, M. J. An, Y. S. Tian, H. J. Chund and B. R. Cho, *Chem. Commun.*, 2012, **48**, 2122-2124.
- 9 D. R. Cary, N. P. Zaitseva, K. Gray, K. E. O'Day, C.B. Darrow, S. M. Lane, T. A. Peyser, J. H. Satcher, Jr., W. P. V. Antwerp, A. J. Nelson and J. G. Reynolds, *Inorg. Chem.*, 2002, **41**, 1662-1669.
- 10 (a) S.-Y. Xu, Y.-B. Ruan, X.-X. Luo, Y.-F. Gao, J.-S. Zhao, J.-S. Shen and Y.-B. Jiang, *Chem. Commun.*, 2010, 5864-5866; (b) D. K. Scrafton, J. E. Taylor, M. F. Mahon, J. S. Fossey and T. D. James, *J. Org. Chem.*, 2008, **73**, 2871-2874.
- 11 (a) K. M. K. Swamy, Y. J. Jang, M. S. Park, H. S. Koh, S. K. Lee, Y. J. Yoon and J. Yoon, *Tetrahedron Lett.*, 2005, **46**, 3453-3456; (b) J. N. Camara, J. T. Suri, F. E. Cappuccio, R. A. Wessling and B. Singaram, *Tetrahedron Lett.*, 2002, **43**,

- 1139-1141; (c) S. Arimori, L. I. Bosch, C. J. Ward and T. D. James, *Tetrahedron Lett.*, 2001, **42**, 4553-4555; (d) L. I. Bosch, M. F. Mahon and T. D. James, *Tetrahedron Lett.*, 2004, **45**, 2859-2862; (e) K. Mulla, P. Dongare, N. Zhou, G. Chen, D. W. Thompson and Y. Zhao, *Org. Biomol. Chem.*, 2011, **9**, 1332-1336; (f) J. D. Larkin, J. S. Fossey, T. D. James, B. R. Brooks and C. W. J. Bock, *Phys. Chem. A*, 2010, **114**, 12531-12539.
- 12 (a) A. Lippert, G. Van de Bittner and C. Chang, *Acc. Chem. Res.*, 2011, **44**, 793-804; (b) M. C. Y. Chang, A. Pralle, E. Y. Isacoff and C. J. Chang, *J. Am. Chem. Soc.*, 2004, **126**, 15392-15393.
- 13 (a) F. Hu, Y. Y. Huang, G. X. Zhang, R. Zhao, D.Q. Zhang, *Tetrahedron Letters*, 2014, **55**, 1471-1474; (b) Y. F. Huan, Q. Fei, H. Y. Shan, B. J. Wang, H. Xu and G. D. Feng, *Analyst*, 2015, **140**, 1655-1661; (c) M.-S. Steiner, A. Duerkop and O. S. Wolfbeis, *Chem. Soc. Rev.*, 2011, **40**, 4805-4839.
- 14 M. Kaur, D. S. Yang, K. Choi, M. J. Cho and D. H. Choi, *Dyes and Pigments*, 2014, **100**, 118-126.
- 15 B. C. Zhu, H. L. Jiang, B. P. Guo, C. X. Shao, H. F. Wu, B. Du and Q. Wei, *Sens. and Actuat. B: Chem.*, 2013, **186**, 681-686.
- 16 V. Stepankova, S. Bidmanova, T. Koudelakova, Z. Prokop, R. Chaloupkova and J. Damborsky, *ACS Catal.*, 2013, **3**, 2823-2836.
- 17 F. Hu, Y. Y. Huang, G. X. Zhang, R. Zhao and D. Q. Zhang, *Tetrahedron Letters* 2014, **55**, 1471-1474.
- 18 Y. F. Huan, Q. Fei, H. Y. Shan, B. J. Wang, H. Xua and G. D. Feng, *Analyst*, 2015,

- 140**, 1655-1661.
- 19 Y. Yi, J. Deng, Y. Zhang, H. Li and S. Yao, *Chem. Commun.*, 2013, **49**, 612-614.
- 20 X. D. Xia, Y. F. Long and J. X. Wang, *Analytica Chimica Acta*, 2013, **772**, 81-86.
- 21 L. Cao, J. Ye, L. Tong and B. Tang, *Chem.-Eur. J.*, 2008, **14**, 9633 - 9640.
- 22 H. S. Cao, V. Chang, R. Hernandez and M. D. Heagy, *J. Org. Chem.*, 2005, **70**, 4929-4934.
- 23 B. Liu and H. Tian, *Chem. Commun.*, 2005, **25**, 3156-3158.
- 24 A. J. Moro, P. J. Cywinski, S. Kosten and G. J. Mohr, *Chem. Commun.*, 2010, 1085-1087.
- 25 Z. Xu, G. H. Kim, S. J. Han, M. J. Jou, C. Lee, I. Shin and J. Yoon, *Tetrahedron*, 2009, **65**, 2307-2312.
- 26 Z. Xu, X. Qian and J. Cui, *Org. Lett.*, 2005, **7**, 3029-3032.
- 27 W. Sun, W. H. Li, J. Li, J. Zhang, L.P. Du and M.Y. Li, *Tetrahedron*, 2012, **68**, 5363-5367.
- 28 K. Wannajuk, M. Jamkatoke, T. Tuntulani and B. Tomapatanaget, *Tetrahedron*, 2012, **68**, 8899-8904.

Figure captions:

Scheme 1 Synthetic route to compound **1**

Fig. 1 (A) UV-vis absorption spectra of compound **1** before (black line) and after (red line) reaction with H_2O_2 ; (B) Normalized fluorescence spectra of 5 μM compound **1** upon addition of increasing concentration of H_2O_2 (0-400 μM) in PBS solution (50 mM, pH = 7.0). $\lambda_{\text{ex}} = 445$ nm.

Fig.2. Normalized fluorescence spectra of 5 μM compound **1** on interaction with 120 μM glucose in the presence (1) and absence (2) of 10 $\mu\text{g/mL}$ GOx in PBS buffered solution (50 mM, pH = 7.0). $\lambda_{\text{ex}} = 445$ nm.

Scheme 2 Schematic representation of the sensing strategy using the compound **1** for glucose detection.

Fig. 3 Normalized fluorescence changes of the 5 μM compound **1** upon interaction with increasing concentration of GOx in PBS buffered solution (50 mM, pH = 7.0) containing 120 μM glucose. $\lambda_{\text{ex}} = 445$ nm.

Fig. 4 Effect of various pH on normalized fluorescence intensity of 5 μM compound **1** in PBS buffered solution (50 mM, pH = 7.0) containing 120 μM glucose and 10 $\mu\text{g/mL}$ GOx. $\lambda_{\text{ex}} = 445$ nm.

Fig. 5 Time-dependent normalized fluorescence changes of the 5 μM compound **1** upon interaction with 120 μM glucose in PBS buffered solution (50 mM, pH = 7.0) containing 10 $\mu\text{g/mL}$ GOx before (red line) and after (black line) . $\lambda_{\text{ex}} = 445$ nm.

Fig. 6 Effect of various temperature on normalized fluorescence intensity of 5 μM compound **1** in PBS buffered solution (50 mM, pH = 7.0) containing 120 μM glucose

and 10 $\mu\text{g/mL}$ GOx. $\lambda_{\text{ex}} = 445 \text{ nm}$.

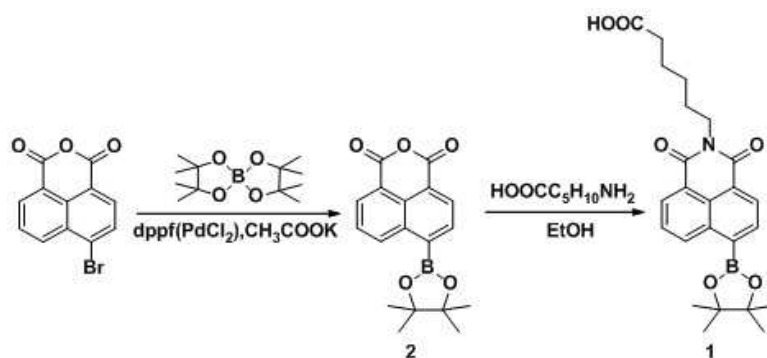
Fig. 7 The relative fluorescence responses of 5 μM compound **1** in PBS buffered solution (50 mM, pH = 7.0) containing 10 $\mu\text{g} / \text{mL}$ GOx, and 120 μM various sugar and biologically relevant species, respectively. $\lambda_{\text{ex}} = 445 \text{ nm}$.

Fig. 8 Normalized fluorescence spectra of 5 μM compound **1** upon addition of increasing concentration of glucose (0-120 μM) in PBS buffered solution (50 mM, pH = 7.0) containing 10 $\mu\text{g/mL}$ Gox. $\lambda_{\text{ex}} = 445 \text{ nm}$. (B) The linear fitting of the normalized intensity vs. glucose concentration.

Fig. 9 The calculated molecular orbitals for compound **1** and **1-H₂O₂**.

Table 1 A comparison of various approaches to glucose detection.

Table 2 Determination of glucose using compound **1** in serum sample (n = 3).



Scheme 1 Synthetic route to compound 1

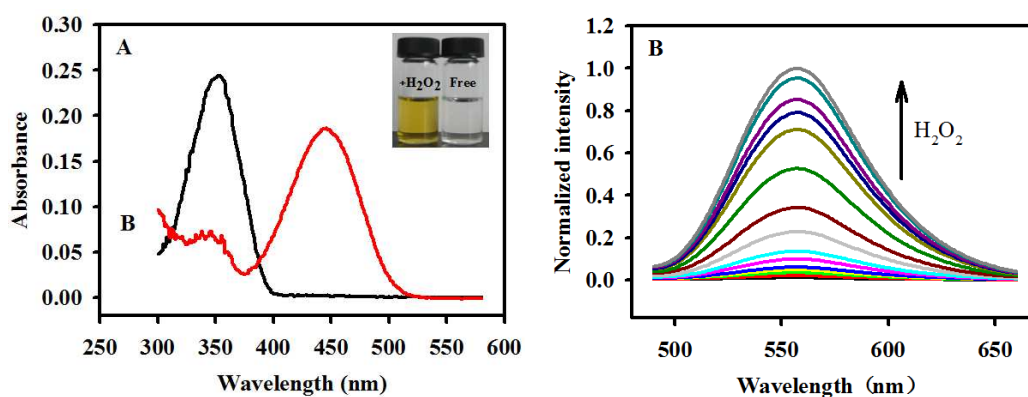


Fig. 1 (A) UV-vis absorption spectra of compound 1 before (black line) and after (red line) reaction with H_2O_2 ; (B) Normalized fluorescence spectra of 5 μM compound 1 upon addition of increasing concentration of H_2O_2 (0-400 μM) in PBS solution (50 mM, pH = 7.0). $\lambda_{\text{ex}} = 445$ nm.

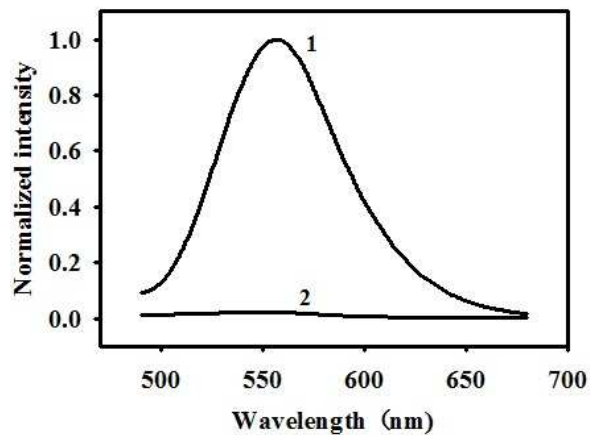
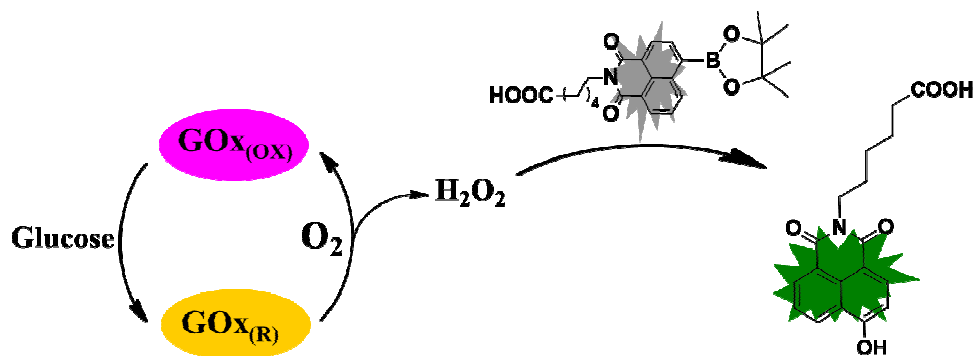


Fig.2. Normalized fluorescence spectra of 5 μM compound **1** on interaction with 120 μM glucose in the presence (1) and absence (2) of 10 $\mu\text{g/mL}$ GOx in PBS buffered solution (50 mM, pH = 7.0). λ_{ex} = 445 nm.



Scheme 2 Schematic representation of the sensing strategy using the compound **1** for glucose detection.

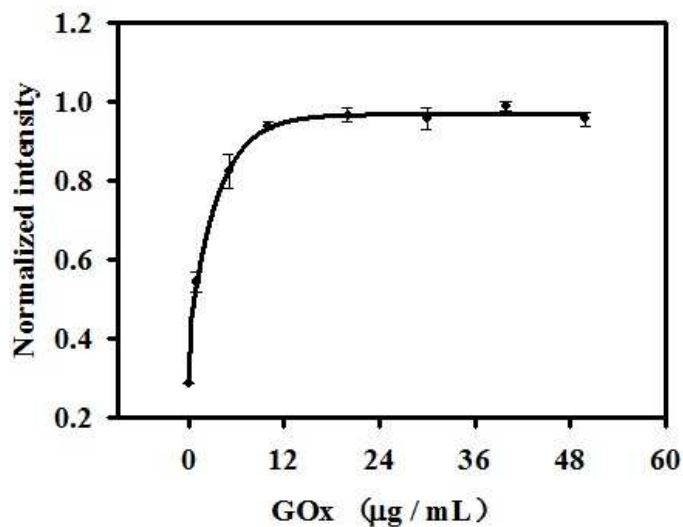


Fig. 3 Normalized fluorescence changes of the 5 μM compound **1** upon interaction with increasing concentration of GOx in PBS buffered solution (50 mM, pH = 7.0) containing 120 μM glucose. $\lambda_{\text{ex}} = 445$ nm.

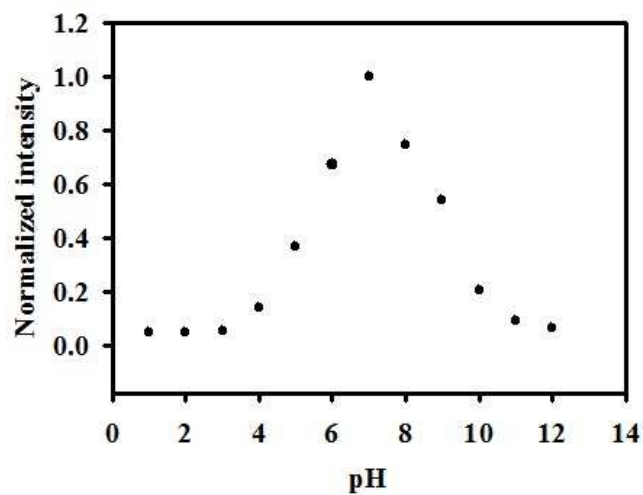


Fig. 4 Effect of various pH on normalized fluorescence intensity of 5 μM compound **1** in PBS buffered solution (50 mM, pH = 7.0) containing 120 μM glucose and 10 $\mu\text{g}/\text{mL}$ GOx. $\lambda_{\text{ex}} = 445$ nm.

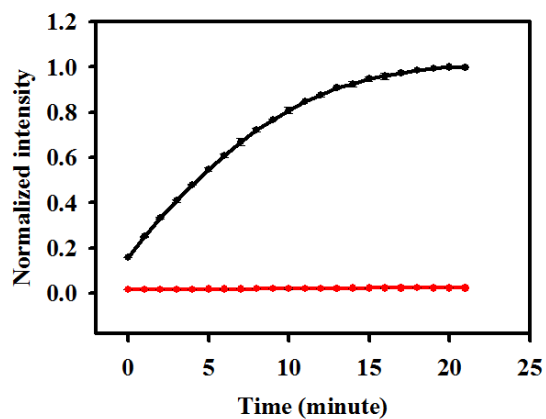


Fig. 5 Time-dependent normalized fluorescence changes of the 5 μM compound **1** upon interaction with 120 μM glucose in PBS buffered solution (50 mM, pH = 7.0) containing 10 $\mu\text{g/mL}$ GOx before (red line) and after (black line). $\lambda_{\text{ex}} = 445$ nm.

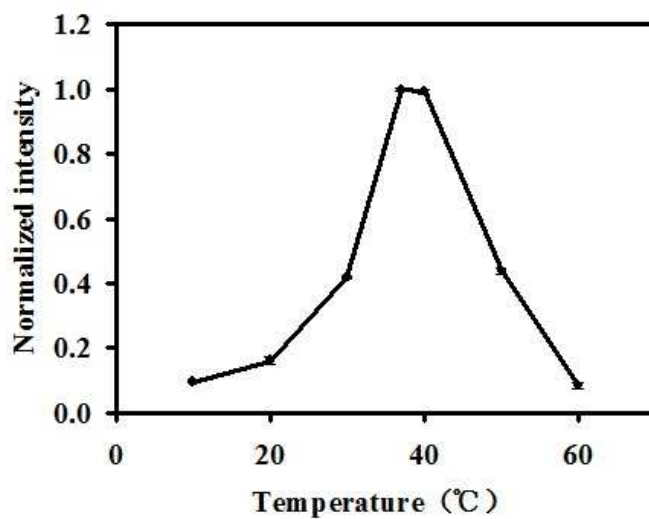


Fig. 6 Effect of various temperature on normalized fluorescence intensity of 5 μM compound **1** in PBS buffered solution (50 mM, pH = 7.0) containing 120 μM glucose and 10 $\mu\text{g/mL}$ GOx. $\lambda_{\text{ex}} = 445$ nm.

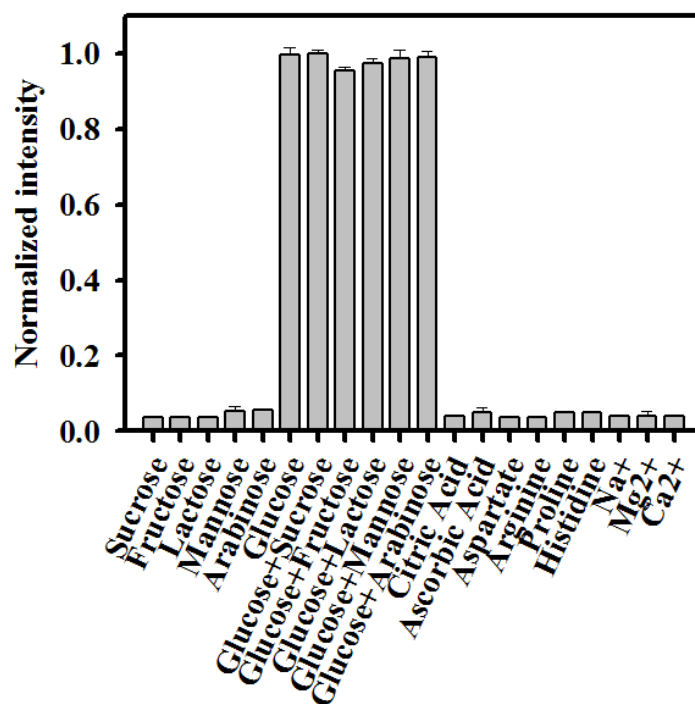


Fig. 7 The relative fluorescence responses of 5 μM compound **1** in PBS buffered solution (50 mM, pH = 7.0) containing 10 $\mu\text{g} / \text{mL}$ GOx, and 120 μM various sugar and biologically relevant species, respectively. $\lambda_{\text{ex}} = 445 \text{ nm}$.

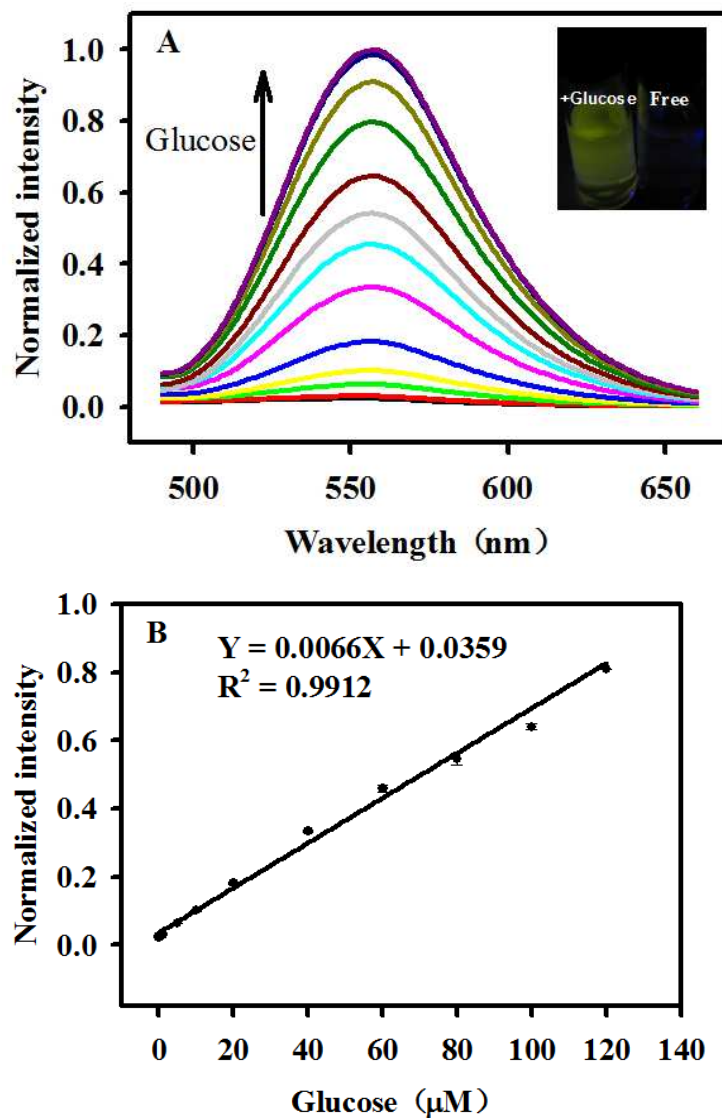


Fig. 8 Normalized fluorescence spectra of 5 μM compound 1 upon addition of increasing concentration of glucose (0-120 μM) in PBS buffered solution (50 mM, pH = 7.0) containing 10 $\mu\text{g/mL}$ Gox. $\lambda_{\text{ex}} = 445$ nm. (B) The linear fitting of the normalized intensity vs. glucose concentration.

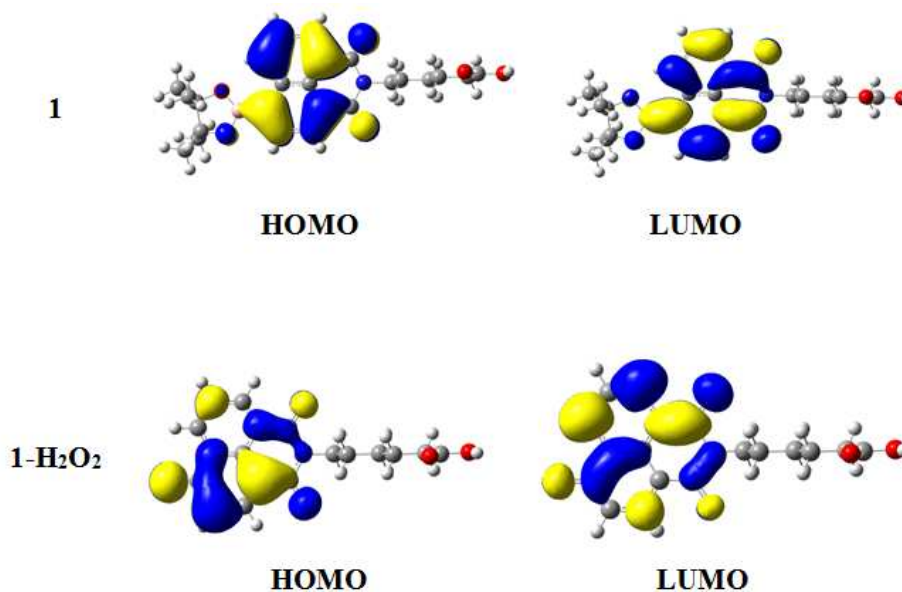


Fig. 9 The calculated molecular orbitals for compound **1** and **1-H₂O₂**.

Table 1 A comparison of various approaches to glucose detection

Method	System	Linear range (μM)	Detection limit (μM)	Ref.
Fluorometry	Tetraphenylethylene / GOx	50 - 250	3	[17]
Fluorometry	Si QDs / GOx	5 - 650	0.68	[19]
Fluorometry	HAQB / GOx	80 - 420	11	[28]
Fluorometry	CdTe QDs / GOx	5 - 1000	0.1	[21]
Fluorometry	Gold nanoclusters / GOx	2.0 - 140	0.7	[20]
Fluorometry	H ₂ TEHPPS / GOx	0 - 5	0.32	[18]
Fluorometry	Naphthalimide / GOx	0 - 120	0.3	This work

Table 2 Determination of glucose using compound **1** in serum sample (n = 3)

Serum samples ^a	Determined (mM)		Added glucose (μ M)	Recovery (%)	RSD (%)
	Compound 1	Hospital instrument			
1	7.43	8.12	30	102.7	4.36
2	5.48	6.20	30	98.6	1.69
3	5.16	5.74	30	93.7	2.83
4	5.01	5.38	30	104.3	1.12

^a Serum samples were diluted 100-folds